

Astronomical Coronagraphy with High Order Adaptive Optics

James P. Lloyd^a, James R. Graham^a, Paul Kalas^a, Ben R. Oppenheimer^a
Anand Sivaramakrishnan^b, Russell Makidon^b, Bruce A. Macintosh^c, Claire Max^c
Pierre Baudoz^d, Jeff Kuhn^d, Dan Potter^d

^aDepartment of Astronomy, University of California, Berkeley, CA 94720

^bSpace Telescope Science Institute, Baltimore, MD 21218

^cLawrence Livermore National Laboratory, Livermore, CA 94551

^dInstitute for Astronomy, University of Hawaii, Manoa, HI 96822

ABSTRACT

Space surveillance systems have recently been developed that exploit high order adaptive optics systems to take diffraction limited images in visible light on 4 meter class telescopes. Most astronomical targets are faint, thus driving astronomical AO systems towards larger subapertures, and thus longer observing wavelengths for diffraction limited imaging at moderate Strehl ratio. There is, however, a particular niche that can be exploited by turning these visible light space surveillance systems to astronomical use at infrared wavelengths. At the longer wavelengths, the Strehl ratio rises dramatically, thus placing more light into the diffracted Airy pattern compared to the atmospheric halo. A Lyot coronagraph can be used to suppress the diffracted light from an on axis star, and observe faint companions and debris disks around nearby, bright stars. These very high contrast objects can only be observed with much higher order adaptive optics systems than are presently available to the astronomical community. We describe simulations of high order adaptive optics coronagraphs, and outline a project to deploy an astronomical coronagraph at the Air Force AEOS facility at the Maui Space Surveillance System.

Keywords: Infrared, Astronomical Instrumentation, Adaptive Optics

1. INTRODUCTION

For the first time in history, astronomers can image the environments of nearby stars on scales comparable to our solar system. New classes of astrophysical objects have been discovered including circumstellar debris disks, brown dwarfs, and super-Jupiter mass planets. These discoveries have galvanized intense public interest in science and technology and have led to profound new insights into the formation and evolution of planetary systems such as our own.

Among the key enabling technologies are adaptive optics (AO) and coronagraphy which deliver the high contrast necessary for the discovery and characterization of faint stellar companions and circumstellar disks in the solar neighborhood. The combination of these two techniques is a powerful technique to study the nearby environment of stars.

The highest order AO system available to the astronomical community is the Air Force AEOS system. This system, coupled with a coronagraph and infrared camera has the potential to achieve studies of the faint companions and circumstellar environment to nearby stars.

2. ADAPTIVE OPTICS FOR SPACE SURVEILLANCE AND ASTRONOMY

Adaptive optics has been developed extensively for space surveillance applications, and more recently applied to astronomy. AO consists of a closed loop control system with a wavefront sensor to measure atmospherically induced wavefront aberrations and a deformable mirror to correct them. The wavefront must be sensed on spatial scales smaller than the coherence length, r_0 , and faster than the coherence time, τ_0 . Thus AO requires a reference source

Send correspondence to James Lloyd, E-mail: jpl@astron.berkeley.edu

Simulated infrared AO coronagraph point spread functions

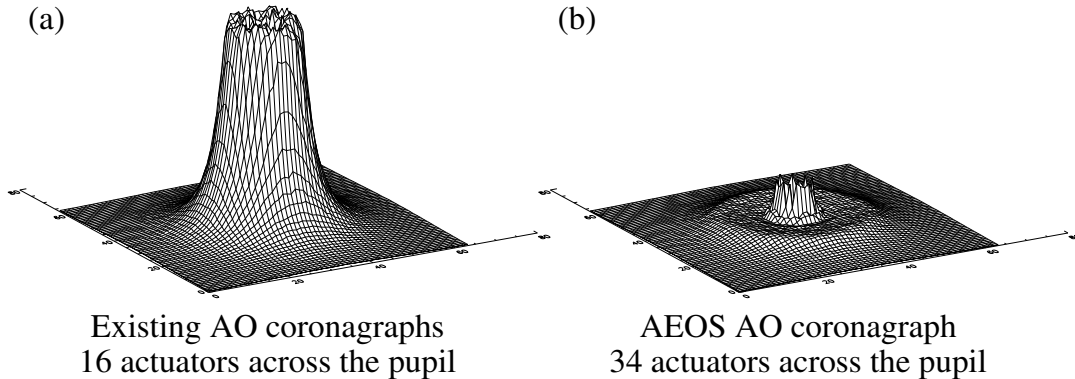


Figure 1.

This simulation demonstrates the halo clearing effect of large AO systems. Suppression of the light in the halo with a large AO control radius allows dramatically increased sensitivity in the immediate environment of the star.

bright enough to provide an adequate supply of photons in the coherence volume, $\pi r_0^2 c \tau_0$. The optical path delay introduced by the atmosphere is essentially achromatic in physical length. Therefore r_0 and τ_0 (and consequently the coherence volume) increase with wavelength as they depend on phase. The required brightness for a guide star is significantly decreased at longer wavelengths, with compromise in angular resolution. The corrected field of view of an AO system is limited by the angle over which the light passes through atmosphere with the same optical properties, which scales with r_0/h , where h is the characteristic height of the turbulence. For a natural guide star AO system sky coverage increases dramatically at longer wavelengths due to the combination of the increased abundance of available guide stars, and increased corrected field of view about those stars. Performance of an AO system is usually characterized by the Strehl ratio, the ratio of the on axis peak intensity to the on axis peak intensity of a perfect image. The extended Marechal approximation,¹ expresses the Strehl ratio, $S = \exp(-\sigma^2)$ as a function of the wavefront phase variance, σ^2 . Strehl ratios approaching one therefore require the wavefront phase to be controlled to a very high precision. These considerations, coupled with the substantial costs of large actuator count AO systems, have driven most astronomical AO systems towards optimization for moderate correction (Strehl $\gtrsim 0.3$) at a wavelengths from 1.0–2.4 μm . At these wavelengths, the atmosphere is transparent at a good site, large format array detectors have recently become available, and interesting science can be done since this wavelength is near the peak of the emission for a 3000K object, similar to the bulk of stars in our galaxy.

Space surveillance requirements, however, have different considerations, that have driven the construction of AO systems for imaging at visible wavelengths to achieve the highest possible resolution of objects illuminated with a solar spectrum, which peaks in the visible.

Naively, once a Strehl ratio becomes a significant fraction of one (say 50%), there is not a large gain in terms of additionally concentrating energy by achieving higher Strehl ratios at the substantial cost of a much higher order AO system. However, for the case of imaging the immediate environment of a star at high contrast, the $1 - S$ fraction of the light that is not controlled by the AO system constitutes a noise background obscuring the immediate environment of the star from study. Due to the typical distance of stars from us, the stellar environment on the scale of our own solar system occurs within this seeing halo.

3. HIGH ORDER AO CORONAGRAPHS

AO increases angular resolution and more importantly contrast, so that a faint object can be detected close to a bright source that would otherwise overwhelm it. To quantify the astronomical utility of high order AO coronagraphy we consider two factors: the degree of contrast enhancement; the radii at which enhanced contrast is achieved (AO Control Radius).

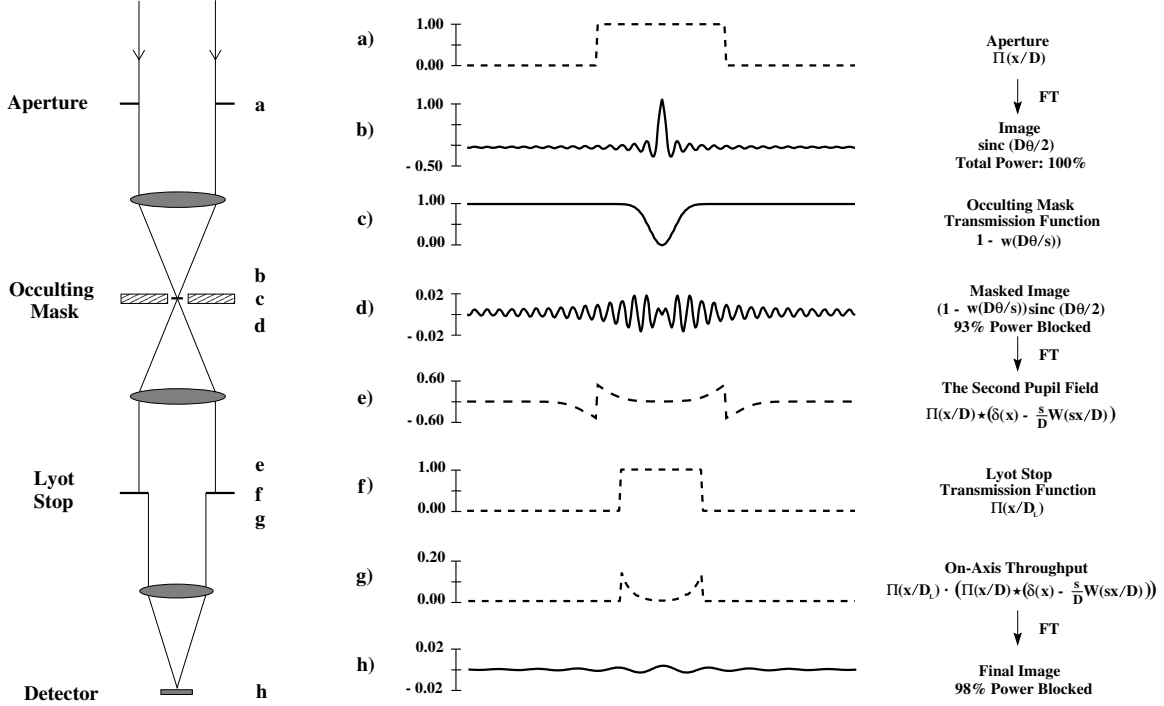


Figure 2. One-dimensional coronagraph summary, with locations and electric field or stop profiles of (a) primary pupil for on-axis source, (b) image before image plane stop, (c) image plane stop, (d) image after image plane stop, (e) pupil before Lyot stop, (f) Lyot stop, (g) pupil after Lyot stop, and (h) final on-axis image. In this example, 98% of the incident power is blocked by the coronagraph.

3.1. Contrast Enhancement

Consider the contrast improvement when an AO system is used to observe two stars which lie within the seeing disk, but outside the Airy disks. Suppose S_{AO} and S_{see} are the Strehl ratios in corrected and uncorrected images. A useful measure of the contrast improvement, η , is the product of two factors: the ratio S_{AO}/S_{see} , due to sharper images; and a factor, $1/(1 - S_{AO})$, which represents the amount of light removed by AO from the seeing disk. Hence,

$$\eta = \frac{S_{AO}}{S_{see}} \frac{1}{(1 - S_{AO})}. \quad (1)$$

For typical astronomical AO systems, e.g., Palomar or Lick, $S_{AO} \simeq 0.5$ and $S_{see} \simeq 0.03$, and $\eta \simeq 30$. For low Strehls image sharpness is the dominant factor. But as $S_{AO} \rightarrow 1$ large improvements accrue as progressively more light is removed from the seeing disk. The AEOS system has enormous astronomical potential because we predict that it can deliver $S_{AO} \simeq 0.93$ in the near-IR at $1.6 \mu\text{m}$ and give $\eta \gtrsim 500$. This advantage diminishes at shorter wavelengths due to the lower Strehl ratio. This steep wavelength dependence, together with our desire to find cool ($T \lesssim 1000 \text{ K}$) companions drives the requirement to equip AEOS with an IR-sensitive array.

3.2. AO Control Radius

The full improvement in contrast exists only within a radial distance from the star, θ_{AO} , which is determined by the design of the AO system. AO correction can be thought of a high pass filter acting on spatial phase variations of incoming wavefronts. The AO system's spatial frequency cutoff is $k_{AO} = N_{act}/2D$, where N_{act} is the number of deformable mirror actuators projected across the primary of diameter D . The electric field at the image and pupil planes are a Fourier pair, so k_{AO} corresponds to an angle $\theta_{AO} = N_{act}\lambda/2D$ on the sky at wavelength λ . Thus AO only improves the point spread function (PSF) within a radius θ_{AO} . The Lick 3-m, Palomar 5-m, and AEOS 3.66-m systems have 8, 16 and 34 actuators across the entrance pupils. Thus AO improves a stellar image to distances of 4 ($0''.4$), 8 ($0''.5$) and 17 ($1''.5$) diffraction widths respectively (cf. Fig. 1).

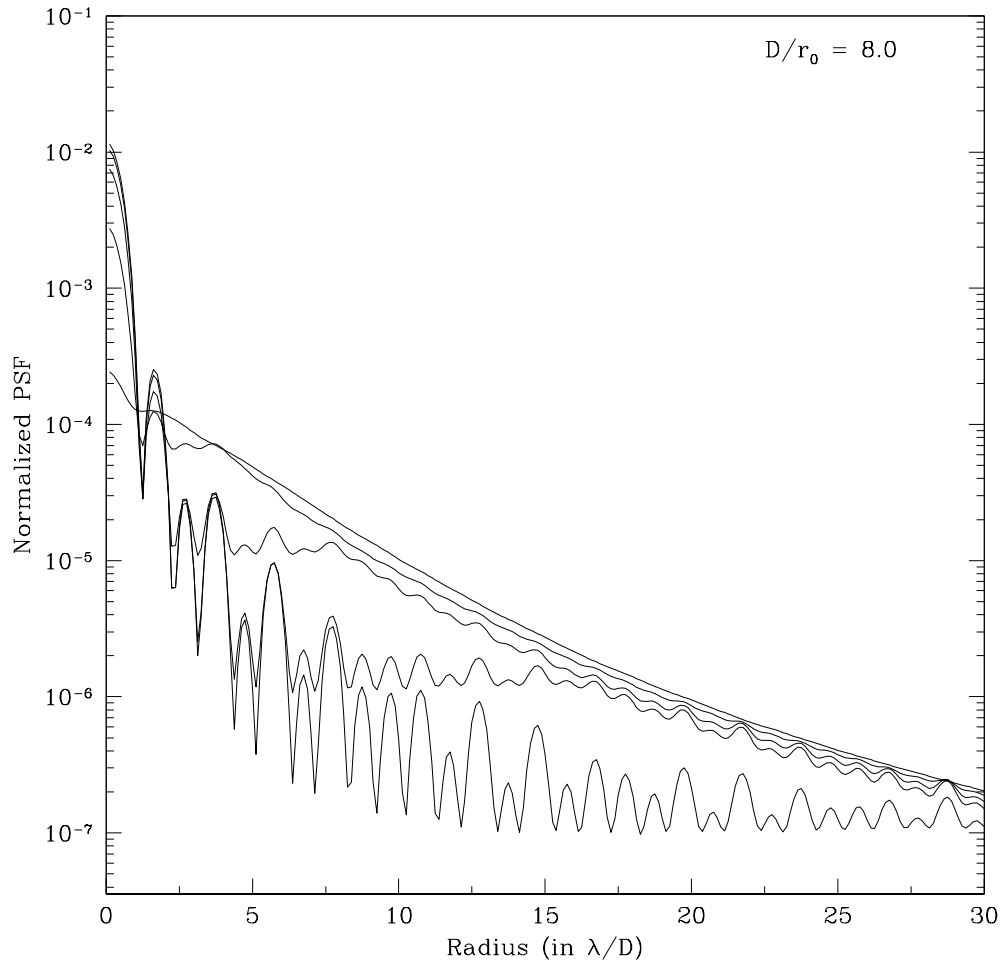


Figure 3. Radial profiles for model AO point spread functions. Effect of increasing AO correction; the same 100 independent realizations of a Kolmogorov spectrum phase screen representing atmospheric wave front aberration corrected by AO systems with 4, 8, 16, 32 and 64 actuators across an 3.6m primary mirror, with $D/r_0 = 8$ (median seeing at AEOS at $1.6 \mu\text{m}$ observing wavelength). The Strehl ratios are 0.05, 0.23, 0.63, 0.87, and 0.96, respectively. Note the widening plateaus of partial correction extending to the shoulder at a distance of $\theta_{AO} = N_{act}\lambda/2D$ from the center of the PSF. Outside this plateau AO correction does not improve the image significantly.

3.3. Coronagraphy

Our science demands high contrast on angular scales corresponding to solar system dimensions (10-30 AU) for nearby stars (10-30 pc) or within the seeing disk at radii of about $1''$. *AO alone cannot achieve the very high dynamic range necessary to find faint companions and circumstellar disks.* This requires a coronagraph. A coronagraph,² consists of two stops placed in the reimaged focal and pupil planes (Fig. 2) respectively. The focal plane stop (Fig. 2(c)) is an opaque disk, usually 3 to 9 times the size of the core of the stellar image. This mask blocks most of the on-axis starlight. The effect of this mask on (b) is shown in (d). After the occulting mask, the pupil is reimaged (e), where the remaining starlight is distributed as the Fourier transform of (d). This light is associated with the Airy rings of the image in a periodic spatial distribution; its periodicity is of the order of the telescope's angular resolution (λ/D). Thus, this energy appears only in an annulus at the edges of the pupil, at a radius of $D/2$ from the center (e). The undersized Lyot stop (f) removes this light at the expense of some reduction of the telescope collecting area. In essence, the Lyot stop is a spatial filter that removes the high spatial frequency components of the electric field. Central obscuration scatters light into a similar bright ring around the inner edge of the pupil. The Lyot stop must mask this too, so that the small AEOS secondary is a great advantage. On AEOS an optimized coronagraph lets up to 34% more light through than on a typical telescope with a secondary diameter a third of that of the primary. The net result is that an on-axis source behind the aperture mask is suppressed by several orders of magnitude relative to an off-axis target.

3.4. Simulations

In order to quantify the potentially large gains that are available with AO coronagraphy, we have simulated the performance of existing (and future) AO systems and coronagraphs.³ An idealized AO system performs as a high pass filter on the atmospheric phase aberrations, by removing all aberrations on larger scales than the subaperture size. The coronagraph can only suppress the light that is made spatially coherent by the AO system and needs to be tailored to the parameters of a given telescope and AO system. Therefore, we have simulated the performance of the AO system and coronagraph as a pair. Fig. 3 shows the output of some radial profiles of simulated AO system point spread functions.

In an optimized coronagraph the occulting spot must span at least four diffraction widths in diameter, since smaller spots require unacceptably undersized Lyot masks (Fig. 2). This results in little gain from using a coronagraph with AO systems where $N_{act} < 8$, since the occulting spot occludes most of the improved image area! At Palomar, with a $5\lambda/D$ ($0''.34$ at $1.6 \mu\text{m}$) radius spot, an improved image annulus of only $3\lambda/D$ wide ($0''.20$) surrounds the spot. For AEOS the image is corrected out to $1''.5$ (at $1.6 \mu\text{m}$). Thus using the smallest coronagraphic masks, the light from the central star is suppressed from the edge of the stop at $0''.2$ to $1''.5$ where AO stops improving the image.

4. HIGH CONTRAST SCIENCE

The science of faint companions of nearby stars relates to many astronomical subfields, including the initial mass function, dark matter, stellar evolution, planet formation and the mounting effort to directly detect extrasolar planets. Presently planetary objects have only been detected indirectly with the radial velocity method, which requires a long time baseline and is relatively insensitive to outer planets. Astrometry, with either ground based interferometers, or the Space Interferometry Mission⁵ offers great promise for indirect detection of planets, but also suffers from the long temporal baseline required to detect outer companions. Direct imaging with a coronagraph requires only sufficient temporal baseline to ascertain physical association by common proper motion. Figure 4 illustrates the relative search space of these (prior and future) techniques sensitivity to low mass companions.

Dust around main sequence stars is the most detectable component of an extrasolar planetary system because of its large cumulative surface area. The Infrared Astronomical Satellite (IRAS) and the Infrared Space Observatory (ISO) show that $>15\%$ of nearby main sequence stars have circumstellar dust that is replenished by the erosion of unseen bodies such as asteroids and comets.⁶ These data indirectly indicate that planet formation may be common, but establishing physical links between circumstellar dust and planet formation demands high resolution coronagraphic imaging.⁷

The AEOS coronagraph will enable the mapping of circumstellar dust structure a few tens of AU radius around Solar neighborhood stars. The sensitivity of the AEOS coronagraph will exceed by over one order of magnitude the the current state-of-the-art provided by the HST NICMOS coronagraph used to resolve the HR 4796A dust ring (Schneider et al. 1999). This improvement is significant because the IRAS and ISO data indicate that only a few

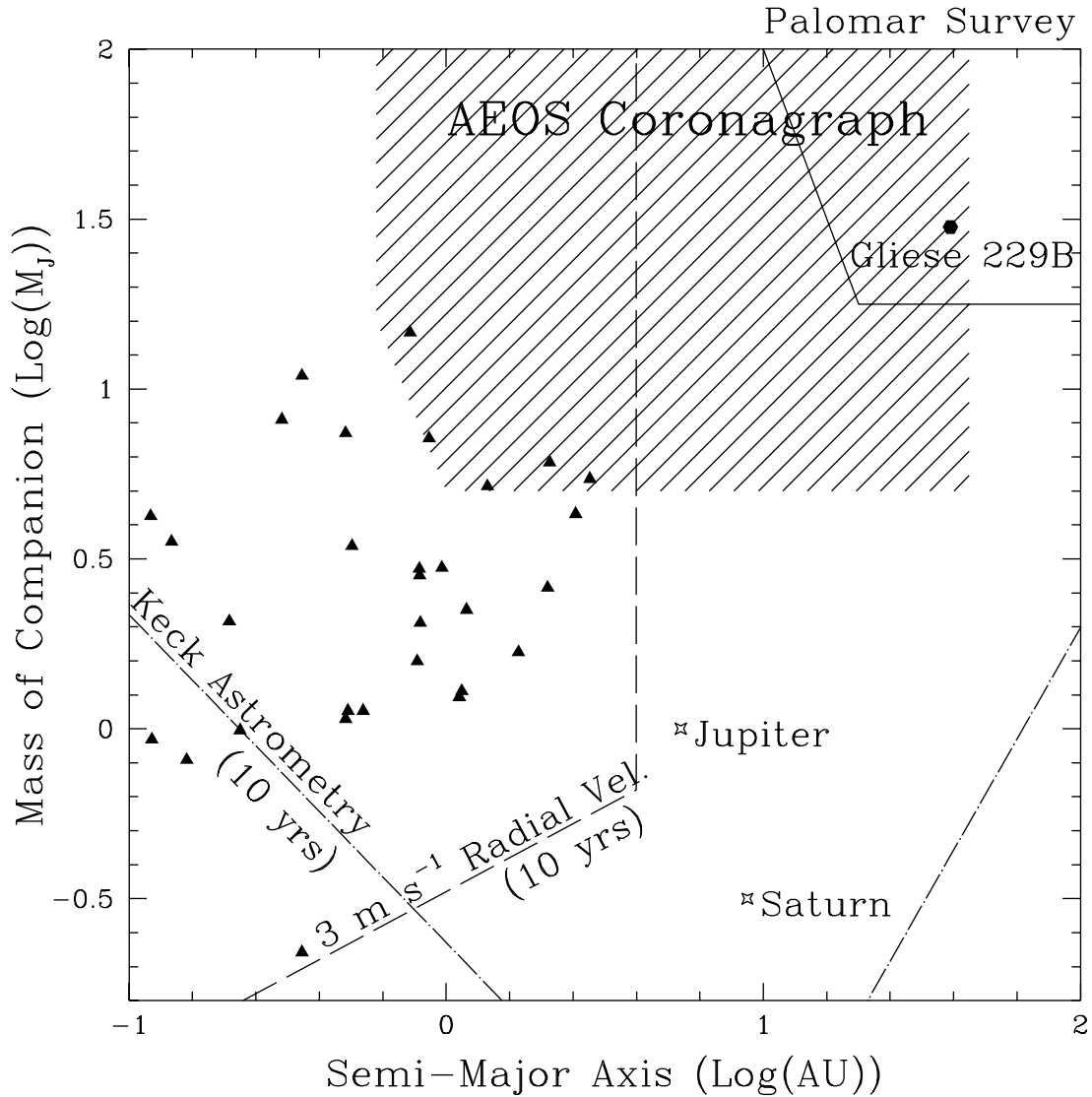


Figure 4. Mass vs. separation parameter space for detection of substellar companions to nearby stars. This space is largely unprobed by direct detection techniques. The 3 m s^{-1} radial velocity searches are limited to the region above the dashed line. Astrometry by the Keck Interferometer is sensitive to objects above the dash-dot line with 10 years of observations. Triangles are indirectly detected objects, and the only directly detected object in this parameter space, Gliese 229B (filled circle), in the trapezoidal region (upper right) probed by Oppenheimer et al.⁴ The region AEOS coronagraphy will probe in our sample of stars is diagonally shaded.

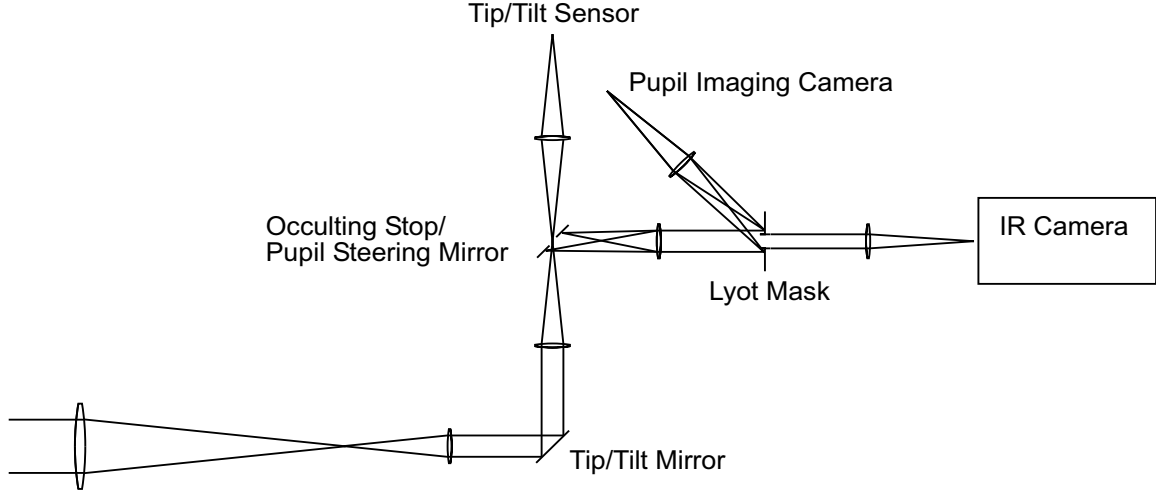


Figure 5. System design for the AEOS coronagraph, incorporating tip/tilt control of the image and pupil positions. The beam entering from the left is the collimated corrected beam from the AEOS AO system.

solar neighborhood stars have dust optical depths as high, $\tau \sim 10^{-3}$, (e.g., HR 4796A and β Pictoris). Rather, nearly 100 stars⁶ including Vega, Fomalhaut, and ϵ Eridani, have $\tau \sim 10^{-5}$, which our simulations indicate will be detectable by the proposed AEOS coronagraph.

Imaging dust disks will achieve two key science goals. First, because extrasolar planets dynamically modify the location of dust, mapping the structure of extrasolar dust disks reveals which nearby stars are likely to have planets in a mass-separation regime that is beyond current radial velocity detection limits. For example, the HR 4796A debris disk⁸ is consistent with the existence of a planet at <60 AU radius that dynamically ejects grains to maintain the empty central region. The greater sensitivity and spatial resolution provided by AEOS will provide reliable maps of dust substructure that will flag perturbing planets.

5. AEOS CORONAGRAPH

To take advantage of the unique capabilities of the AEOS telescope and AO system for astronomical observations, we are constructing a coronagraph and infrared camera. The architecture of the AEOS system, with a central AO system feeding multiple Coudé labs offers a spacious, stable, temperature controlled environment for the coronagraph. Figure 5 indicates the system design for the coronagraph optics. The coronagraph performance is critically dependent on accurately positioning the beam on the occulting spot and Lyot mask. Since there is residual image motion from the AEOS AO system, and vibration of the steering mirror that transfers the beam from the AO system to the Coudé labs, we require a fast tip tilt system. In order to simplify the requirements on the tip tilt mirror, we will compress the 10 cm beam to 40 mm, placing the tip/tilt mirror at the image of the telescope pupil. After forming an image, the occulting spot is accomplished with a hole in a mirror. The light that enters this hole is used to sense the stellar position and control the tip/tilt mirror. The light that reflects off this mirror is recollimated, and an image of the telescope pupil formed at the Lyot mask, which is mounted on a rotation stage to track pupil rotation. The alignment of the beam to the pupil is accomplished by a tip/tilt stage at the occulting mirror, with pupil position sensed with a video camera imaging the Lyot mask. The light exits the coronagraph and is reimaged to an output focal plane. The infrared camera is an Offner image relay,⁹ which forms an image on a cold pupil to block stray thermal radiation. A novel feature of the camera is the use of a reflective filter coated onto the secondary mirror for efficiency and the elimination of ghosts. The detector is a 2048×2048 pixel HgCdTe Hawaii-2 device sensitive from 0.8 to $2.5 \mu\text{m}$,¹⁰ controlled by a fast 32 channel SDSU-2 controller¹¹ capable of coadding full frame readout at 8 Hz. Planned future upgrades include the use of multi-channel polarimetry for psf subtraction,¹² and phase quadrant masking.¹³

6. CONCLUSION

Adaptive Optics offers great potential for studies of the environment of stars, ranging from protostellar and debris disks, low mass stellar and substellar companions, and ultimately planets. In order to detect this faint material, it is necessary to use a coronagraph to remove the light from the on axis star. Successful coronagraphy close to the star requires the highest possible Strehl ratio and the highest order adaptive optics available to clear the seeing halo of incoherent light, which can then be filtered by the coronagraph. The AEOS space surveillance system is the highest order AO system available, and therefore opens the way for new discoveries of the nature of planetary systems around other stars.

ACKNOWLEDGMENTS

J. L. acknowledges the cosponsorship of the Australian-American Educational Foundation (Fulbright Commission) and assistance from the Institute of International Education. This work has been supported in part or full by the National Science Foundation Science and Technology Center for Adaptive Optics, managed by the University of California at Santa Cruz under cooperative agreement No. AST-9876783. A.S and R.M acknowledge funding from the Space Telescope Directors Discretionary Fund. The construction of the coronagraph is partially funded by a joint program between the National Science Foundation and Air Force Office of Scientific Research for first light science with AEOS.

REFERENCES

1. J. W. Hardy, ed., *Adaptive optics for astronomical telescopes*, Oxford University Press, 1998.
2. B. Lyot, "The study of the solar corona and prominences without eclipses (George Darwin Lecture, 1939)," *MNRAS* **99**, pp. 538+, May 1939.
3. A. Sivaramakrishnan, C. D. Koresko, R. B. Makidon, T. Berkefeld, and M. J. Kuchner, "Ground-based coronagraphy with high-order adaptive optics," *ApJ* **552**, pp. 397–408, May 2001.
4. B. R. Oppenheimer, D. A. Golimowski, S. R. Kulkarni, K. Matthews, T. Nakajima, M. Creech-Eakman, and S. T. Durrance, "A coronagraphic survey for companions of stars within 8 parsecs," *AJ* **121**, pp. 2189–2211, Apr. 2001.
5. M. Shao, "Astrometric planetary detection from space," in *IAU Symposium*, vol. 202, pp. E29–+, 2000.
6. D. E. Backman and F. Paresce, "Main-sequence stars with circumstellar solid material - The Vega phenomenon," in *Protostars and Planets III*, pp. 1253–1304, 1993.
7. P. Kalas, "Links between dust disks and exoplanets," *Earth Moon and Planets* **81**, pp. 27–34, 1998.
8. G. Schneider, B. A. Smith, E. E. Becklin, D. W. Koerner, R. Meier, D. C. Hines, P. J. Lowrance, R. J. Terile, R. I. Thompson, and M. Rieke, "NICMOS Imaging of the HR 4796A Circumstellar Disk," *ApJ* **513**, pp. L127–L130, Mar. 1999.
9. A. Offner, "New concepts in projection mask aligners," *Optical Engineering* **14**, pp. 130–132, 1975.
10. C. A. Cabelli, D. E. Cooper, A. K. Haas, L. J. Kozlowski, G. L. Bostrup, A. C. Chen, J. D. Blackwell, J. T. Montroy, K. Vural, W. E. Kleinhans, K. Hodapp, and D. N. Hall, "Latest results on HgCdTe 2048x2048 and silicon focal plane arrays," *Proc. SPIE* **4028**, pp. 331–342, July 2000.
11. R. W. Leach and F. J. Low, "CCD and IR array controllers," *Proc. SPIE* **4008**, pp. 337–343, Aug. 2000.
12. D. Potter, P. Baudoz, O. Guyon, W. Brandner, L. Close, J. E. Graves, and M. Northcott, "A high dynamic range dual imaging polarimetric survey of circumstellar disks around young stars using Gemini North with Hokupa'a," in *American Astronomical Society Meeting*, vol. 198, pp. 1802+, May 2001.
13. D. Rouan, P. Riaud, A. Boccaletti, Y. Clénet, and A. Labeyrie, "The four-quadrant phase-mask coronagraph. I. Principle," *PASP* **112**, pp. 1479–1486, Nov. 2000.